NEURAL NETWORK BASED CONCEPTUALIZATION AND DESIGNOF A TWO-STAGE VIDEO COMPRESSION ARTEFACT REDUCTION STRATEGY

Dr.C.RAVICHANDRAN,
Associate Professor, GRT Institute of Engineering and Technology,
Tiruttani, India, ravisarvajith@gmail.com
Dr.T.THIRUMURUGAN..,
Professor/ ECE Department, Christ College of Engineering and Technology, Puducherry, India
thiru0809@gmail.com
Dr.C.SENTHAMARAI,
Associate Professor/ CSE Department, M.A.M School of Engineering, Trichy, India ,
senthamarai.subbu22@gmail.com
Dr.C.KALAISELVAN,
Professor/ ECE Department, NRI Institute of Technology, Guntur, Andhra Pradesh, India,.
kalaiaswath@gmail.com

ABSTRACT

Multimedia communication has had a huge impact on data transmission and reception in recent years. Video transmission, reception, and storage are all important aspects of multimedia communication. The requirement to store the movie on the drive necessitates a significant amount of space and memory. Lossy compression and lossless compression are the two types of video compression techniques. Lossy compression compresses video frames more efficiently than lossless compression, but the video quality suffers as a result of artefacts. When compressing the video frame, an artefact reduction technique is employed in this study. Despite the fact that video frame data compression techniques have the ability to dramatically reduce the quantity of video frame material, they also generate visual distortions due to lossy compression. The proposed method increases video quality after compression by employing the DREPF technology to remove artefacts. DREPF has been proposed as a way to improve decoded video frames after compression using a technique called Recursive Ensemble Particle Filtering (REPF). Recursive Ensemble Particle Filtering (REPF) locations are determined using the DCNN, which is utilized to include them into the deep Recursive Ensemble Particle Filtering (REPF). For better video frame enhancement, the previous information is approximated by combining the time and temporal systems. Model-based and learning-based systems can be combined in a novel way by combining the Recursive Ensemble Particle model's recursive structure with DCNN's dominating illustration capabilities.

*e*ISSN1303-5150 www.neuroquantology.com

Experiments have shown that the proposed methodology produces better outcomes than current systems.

Keywords: Deep Convolutional Neural Network (DCNN), Deep Recursive Ensemble Particle Filter (DREPF), Lossless compression, Lucy–Richardson (LR) algorithm

DOINumber:10.14704/nq.2022.20.8.NQ44084 **NeuroQuantology2022;20(8):778-790**

1. Introduction

Video compression is a frequent practice in many real-world (especially mobile) application situations because of limited bandwidth and storage capacity [1]. Despite the fact that lossy video compression reduces transmission and storage costs, jerkiness, edge/texture floats, and mosquito noise are all introduced [2]. Because to visual distortions, the quality of the experience can suffer (QoE). Thus, in the disciplines of multimedia and computer vision, video compression artefact reduction has become a prominent topic The successful implementation of deep neural networks has resulted in considerable breakthroughs in compressed image/video enhancement in recent years. Using deep convolutional neural networks, for example [6-9], it is possible to remove compression artefacts from images without having to consider the underlying compression algorithms. There are no temporal links between adjacent frames in these models. Using two motion-compensated closest PQFs, [5] exploits the temporal correlation of adjacent frames to establish a deep Kalman filter network, [10] makes use of task-oriented motions, and [3] introduces the deep Kalman filter network. However, [3] only uses the target frame's preceding frames, whereas [10, 5] only use a pair of nearby frames, potentially missing high-quality features in other neighbor frames (will be explained later). Intra-frame and inter-frame codecs are used in video compression algorithms. The preceding and next neighbor frames have a considerable impact on intercoded frames (P and B frames). So finding spatiotemporal correlations between adjacent frames can improve video enhancement performance. Compression video artefacts can't be minimized by just mining information from one or two neighboring frames or even two close PQFs. Figure 1 illustrates this concept by way of an illustration. SSIM (structural similarity index measure) values above a threshold are indicative of higher visual quality in a frame. In spite of the overall visual quality of the 140th and 143rd frames being greater, the 142nd frame has the best cropped patch. Current approaches to extracting spatiotemporal information from videos would miss the high-quality details in these patches.

Reduction methods for compression artifacts were initially studied by developing a specific filter inside the compression process [11]. Although these approaches can efficiently remove ringing artifacts [12], the improvement in image regions is limited at high frequencies. Examples of such approaches include deblocking-oriented approaches [13,14],wavelet transforms [15,16], and shape-adaptive discrete cosine transforms [17]. Numerous DNNs have been developed in the past few years with the goal of reducing artefacts in machine learning. These DNNs include convolutionary, recurrent and generative adversarial models (GANs). The use of CNN-based artefact reduction (AR) techniques can improve visual performance in terms of peak signal-to-noise ratio (PSNR) [19], PSNR with blocking effects (PSNR-B) [20,21],

and structural similarity index measurements SSIM [22].

Despite the developments of AR, most CNN-based approaches tend to design the heavy network architecture by increasing the number of network parameters and operations. Because it is difficult to deploy such heavy models on hand-held devices operated on low complexity environments, it is necessary to design the lightweight AR networks. A lightweight CNN-based artifacts reduction model is used to reduce the memory capacity as well as network parameters. The main works of this study are summarized as follows:

- To reduce the coding artifacts of the compressed images, we propose a CNN based densely cascading image restoration network (DCRN) with two essential parts, densely cascading feature extractor and channel attention block.
- Through a various ablation study, the proposed network is designed to guarantee the optimal trade-off between the PSNR and the network complexity.
- Compared to the previous method, proposed network is designed to obtain comparable AR performance while utilizing the small number of network parameters and memory size. In addition, it can provide the fastest inference speed, except for initial AR network [30].
- Compared to the latest methods to show the highest AR performances (PSNR, SSIM, and PSNR-B), the proposed method can reduce the number of parameters and total memory size maximum by 2% and 5% respectively

2. Related Works

Several strategies for reducing picture compression artefacts have been proposed. Early efforts like the sparsity-based image restoration algorithms [23, 24] were presented as a starting point for sharpening photographs. Image compression artefacts can be minimized using deblocking-oriented and deep learning-based algorithms.

In order to eliminate ringing and blocking artefacts, deblocking-oriented techniques are employed in the audio industry. The SA-DCT [25] methodology is widely accepted as the most advanced deblocking approach, despite the fact that it, like many other deblocking-oriented algorithms, can produce false results and lose the sharp edges of the original images. In order to minimize blocking artefacts, Wu [26] has presented wavelet transforms based on the Meyer algorithm.

In many circumstances, neural networks and deep learning are now the most viable solutions. Deep learning's ability to provide exact detection and predicting has improved steadily in recent years. Thanks to recent advances in deep learning, picture compression artefacts reduction has made a huge leap forward. As part of their work on image restoration, Dong and his colleagues developed an algorithm with four convolution layers to reduce artefacts due to image compression. [27] Researchers were able to begin training larger and deeper neural networks thanks to GPU performance and optimization methodologies.

In order to remove artefacts from JPEG-compressed images, Wang et al. [28] suggested a Deep Dual-Domain based fast restoration method. In order to take advantage of this, deep networks are utilized. Testing has revealed that the suggested D3 model outperforms current methods. A CNN (IG-Net) model developed by Wang et al. [29] learns to map the intensity picture and distorted depth map to an

uncompressed deep image by learning to map the IG-Net model.

Deep learning techniques such as convolutional neural networks play a critical role in computer vision. For image-related tasks like object detection, unsupervised training of Convolutional Neural Networks (CNN) has become increasingly popular. Optimal CNNs can be trained to penalize the discrepancy between the output image and the ground truth image in order to uncover the mapping between the input image and the reasonable output image. The two CNN models differ greatly in terms of network architecture[36] and loss function parameters[35]. The L2 (or L1) norm can be used to evaluate the outputs pixel by pixel by measuring the distance between the output and ground truth images in pixel space. As a result, the final photographs may appear blurry when they're printed.

generative adversarial networks (GANs) have been used successfully in a large number of applications since they were first described by Goodfellow et al. [33] in 2014. (e.g., SRGAN [30], DCGAN [31], Pix2Pix [32]). There is a difference between what GANs construct and what the real data distribution is, which is examined by generative adversarial losses. Using generative adversarial losses, more "realistic" pictures can be generated. An successful GAN network for compression artefact reduction was inspired by the success of generative adversarial networks (GANs), which we created after learning about their success in image-to-image translation. Our image analysis shows that the recommended networks perform well for us. Our strategy outperforms current best practices in terms of both qualitative and quantitative performance, according to our research.

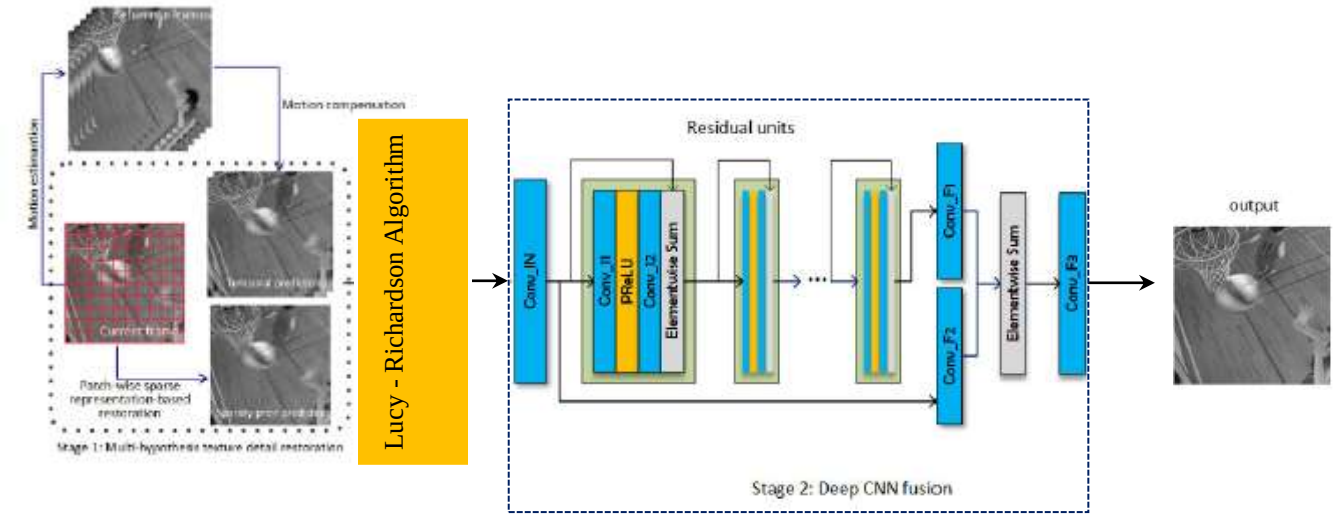

Figure 1**.** Conceptualization and design of a two-stage video compression artefact reduction strategy.

3. Methodology

Fig. 1 displays the suggested artefact reduction strategy, which consists of two stages: 1)

texture detail restoration and 2) deep CNN Fusion (see text for more information). [35] A patch-by-patch strategy to picture restoration is used in the first stage, while a deep CNN is used in the second stage to consolidate previous predictions [35].

3.1 Video Sequence

A video sequence is a timeline including video, audio, and graphics clips that are ready to restore frames. When recognizing duplicate images, a frame changing sequence changes the video correlation. The video sequence establishes the entire process and isolates the frame from the optical flow, which arranges deep frames that change model.

3.2 Lucy Richardson Algorithm

Iterative nonlinear restoration using the Lucy Richardson (LR) technique. Maximizing the likelihood formulation, hazardous statistics are used to model the picture. Iteration after iteration of a model's likelihood function converges when an equation is satisfied:

$$\hat{f}_{k+1}(x,y) = \hat{f}_k(x,y)\left[h(-x,-y) * \frac{g(x,y)}{h(x,y) * \hat{f}_k(x,y)}\right]$$

When employing this strategy, the question of where to end naturally arises. If the PSF matrix is large and complex, it is difficult to estimate the number of iterations required. The approach typically achieves a stable solution quickly with a minimal PSF matrix (in a few steps). However, if you stop after a few iterations, the image will be quite smooth. Increasing the number of iterations, on the other hand, not only slows down the computation, but also amplifies noise and generates the ringing effect. [34] provides several further ringing reduction approaches. As a result, for a "excellent" quality restored image, the appropriate number of iterations is manually chosen for each image based on the PSF size.

3.3 Proposed Modified Lucy Richardson Algorithm

Because the suggested solution uses the DWT of a degraded image, we'll go over the properties of DWT briefly. Similar to human visual system models, DWT's spatial localization and multiresolution features are comparable. DWT decomposes three high-frequency sub-images (HL, LH, and HH) and one low-frequency sub-image into four sub-band images (LL, named approximate sub-image). The exact sub-image is the convergence of the original picture strength, whereas the fine-grained sub-image contains fringe information. For this reason, it is more stable than the detail sub-images. As a result, the LL sub-band image will be subjected to the Lucy Richardson algorithm.

1) Take a non-blurred image of size 512x512.
2) To create a blurry image, use a filter like Gaussian blur or motion blur.
3) Now add Gaussian noise to produce degraded image G.
4) Each of the four DWT sub bands (LL, HL, LH and HH) is 256x256 pixels in size.
5) Apply the LR approach to the LL sub-band and you'll get the restored low frequency band LLM.
6) HL, LH, and HH are the last three photos to be thresholded.
7) DWT is applied to LLM, HL, LH and HH to restore the image $\hat{f}$.

3.4 Deep Convolutional Neural Network (DCNN) for video frame artifact elimination

The deep convolution concept of instruction also increases its capacity for extracting features and its reliability for efficient operation. Until matching, the feature learning

clustering algorithm of a sample picture was retrieved using a computer program. In the suggested DCNN, to predict image quality optimization outcomes, multi-level feature vectors are trained and removed. In this strategy [36], high-level technologies with information dissemination are combined with low-level feature with location data to boost low-light input images.

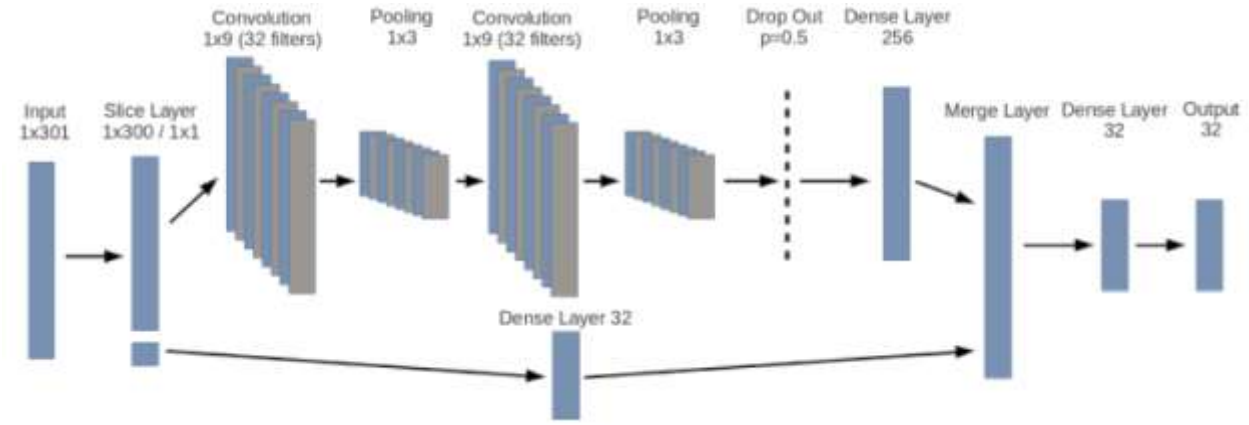

Figure 2 Architecture diagram of Deep Convolutional Neural Network (DCNN)

DCNN's architecture is seen in Figure 2. The suggested network can efficiently spread the differential regression to the previous nodes within the network by terms of long-range residual ties and interfaces. This is of critical significance to our strategy which helps our network to achieve successful end-to-end preparation. The suggested DCNN consists of two convergent path modules: part of the forward encoder and part of the reverse decoder. A 4-cascaded network is modeled in our design, incorporating four sub-nets in the decoder section. The performance of the linked layers in the previous encoding portion is taken as input by both of these sub-networks. Furthermore, the performance of the previous sub-net is also related to the sub-net below. Despite the fact that the architectures of all the sub-networks are identical, the requirements of the sub-networks are not related, allowing versatile adaptation to be carried out by each system. There have been very few experiments employing deep learning approaches for the reconstruction of pictures. For video frame de-noising and post-de-blurring de-noising, multi-layer perception (MLP), whose all levels are completely (as opposed to convolutional), is implemented. For video frame de-noising and elimination of noisy variations, the convolutional neural network has been more intimately associated to our function. Almost de-noising-driven are these reconstruction issues. On the opposite, the object super-resolution concern has not experienced to the best of knowledge the use of deep learning methods.

Create a single video frame that is low-resolution. With recurrent connections, which is really the only pre-processing we do, we first upgrade it to the required level. Y is the name given to the resampled object. An image F(Y) that closely resembles the elevated view of the ground reality X is what we are trying to get out of the input data set Y. Although Y is the same size as X, we name it a "low-resolution" image

for convenience's sake. F is a three-step process that we'd like to master.

4. Results & Discussion

Digital image processing uses the Lucy–Richardson (LR) algorithm, a nonlinear image restoration procedure. Bayesian reconstruction methods are used. You can better comprehend the Lucy-Richardson (LR) deconvolution approach by first examining how an iterative process works, and then by comparing the two methods.

The linear imaging equation states that $g(x,y) = f(x,y) ** h(x,y) + n(x,y)$, so that the noise $n(x,y)$ is the difference between the output distribution $g(x,y)$, (i.e. picture we really took) and the uncertain distribution of input signals $f(x,y)$ convolved with the PSF $h(x,y)$:

$$n(x,y) = g(x,y) - f(x,y) ** h(x,y). \quad (3)$$

Use of an accurate prediction of the input distribution instead of the original $f(x,y)$ in Equation (3) would tend to make $n(x,y)$ it is tiny, whereas a poor estimate would make it huge, and in the limit of low noise, our ideal estimate would meet

$$g(x,y) - f(x,y) ** h(x,y) = 0\,. \quad (4)$$

If we add the input distribution $f(x,y)$ to both sides of Equation (4), then we have

$$f(x,y) = f(x,y) + [g(x,y) - f(x,y) ** h(x,y)]. \quad (5)$$

One way to think of this equation is as a combination of the prior estimate (first term on the right-hand side) and a correction term to get an updated estimation of the input (left-hand side) (in brackets). What we call "correction" here refers to the difference between our actual image and our best guess at the original input. This appears to be a sensible change, as well as a straightforward one to calculate. By explicitly stating this as an iterative operation, we get the (k+1)th estimate of the input

$$f_{k+1}(x,y) = f_k(x,y) + [g(x,y) - f_k(x,y) ** h(x,y)]. \quad (6)$$

Equation (6) describes how to begin the method by setting Alternatively, we seed the algorithm by estimating the input distribution based on what we measured. Unless the image is substantially deformed, you should be able to get good results with the deblurring method. For varying the rate of convergence of Equation (6), the Van Cittert approach applies a pixel-dependent weighting factor or relaxation parameter:

$$f_{k+1}(x,y) = f_k(x,y) + w(x,y)[g(x,y) - f_k(x,y) ** h(x,y)]. \quad (7)$$

A Bayesian technique is used by Lucy-Richardson (LR), an iterative programme that attempts to restore images. Alternatively, Equation (7) can be written as follows:

$$\hat{f}_{k+1}(x,y)=\hat{f}_k(x,y)\left[h(-x,-y)*\frac{g(x,y)}{h(x,y)*\hat{f}_k(x,y)}\right] \quad (8)$$

Only if there is no noise at all can the correction term in Equation (8) be reduced to its minimum value, as illustrated in Equation (9) (3). The mean square error (MSE) is 2.4.

The impact of picture restoration was assessed by calculating the MSE, or mean square error. The following is how the MSE is described:

$$MSE=\frac{1}{M\times N}\sum_{x=1}^{M}\sum_{y=1}^{N}[o(x,y)-r(x,y)]^2. \quad (9)$$

Where $o(x,y)$ is the matrix representing the original image, $r(x,y)$ is the matrix that represents the restored image matrix's The matrix size is represented by the parameters M and N $o(x,y)$ and $r(x,y)$ respectively.

4.1 Numeric simulation experiment

Gaussian model was used to create the motion blurring image. The original PSF and a new PSF that differed from the original were used in the image restoration parameters. Table 1 and Table 2 show PSF kinds 1 and 2, respectively. In Figure 3, you can see a restored version of the PSF. A variety of iteration lengths are employed.

Table 1 The MSE of restoration image with the original PSF

Irrelative times	5	10	15	20	25	30
MSE	0.2311	0.2460	0.2609	0.2648	0.2668	0.2682

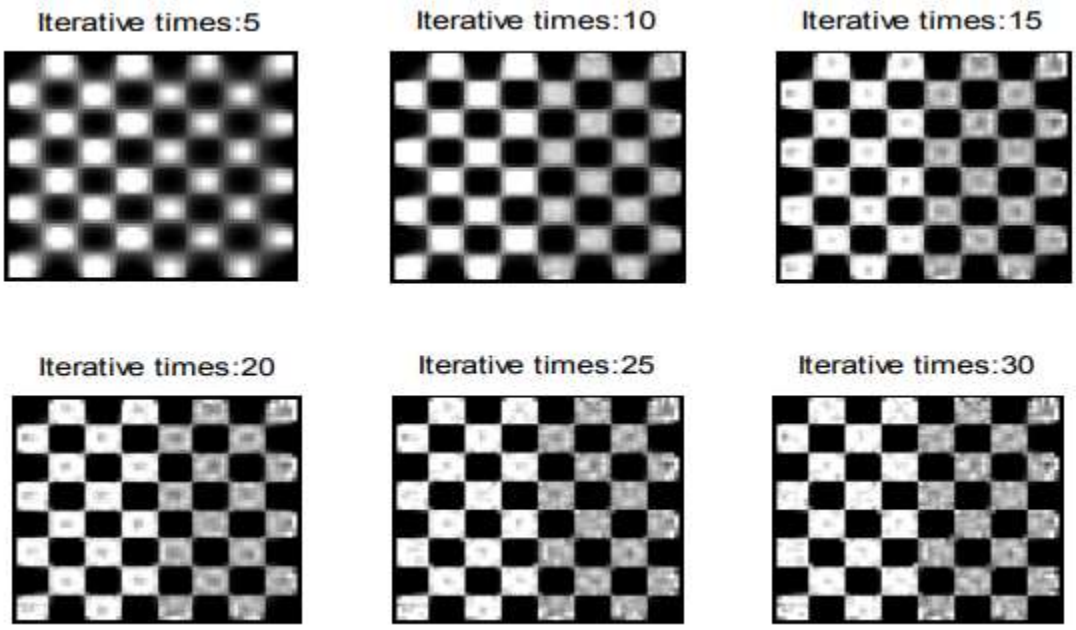

Figure 3: the original PSF was used to restore the image many times during the restoration processThe restoration image of the various PSFs is shown in Figure 4. Table 2 illustrates the MSE for various PSFs. It can be seen that the MSE increases as the data in table 1 increases.

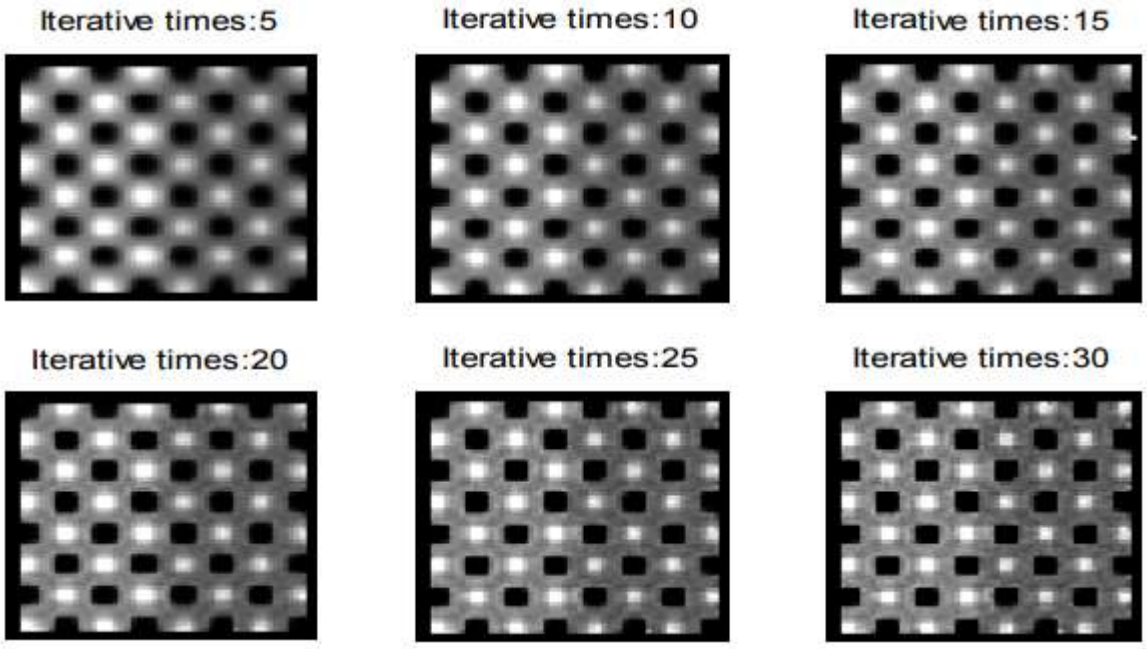

Figure 4: a different PSF for each iteration of the restoration process

Table 2 The MSE of restoration image with different PSF

Irrelative times	5	10	15	20	25	30
MSE	0.3101	0.3263	0.3354	0.3472	0.3501	0.3511

The proposed approach is based on a grayscale image with a dimension of 512 x 512 pixels. The proposed method was put to the test in the presence of Gaussian and motion blur. There are two performance evaluation metrics known as PSNR and MSE, which are defined as follows:

$$\text{PSNR(dB)} = 10\log_{10}\frac{255\times255}{MSE}\&\text{MSE} = \frac{1}{M*N}\sum_{x=1}^{M}\sum_{y=1}^{N}\left(f(x,y)-\hat{f}(x,y)\right)^2$$

Where M X N signifies the image size $f(x,y) and\ \hat{f}(x,y)$ and pixel values at the (x,y)th location of the original and restored images, respectively. Original and repaired pictures were tested for resemblance using PSNR (percentage similarity ratio). Higher PSNR and lower MSE can be achieved with better deblurring.

Figure 1 shows a clear image, but Figure 2 shows a fuzzy and noisy image with Gaussian noise. As can be seen in the images in Figures 3 and 4, the recovered images were created using several techniques, including the wiener filter, CLS, LR, and the modified LR method with Gaussian Blur. Figures 5 and 6 show the restored images created with the LR method and CLS, respectively.

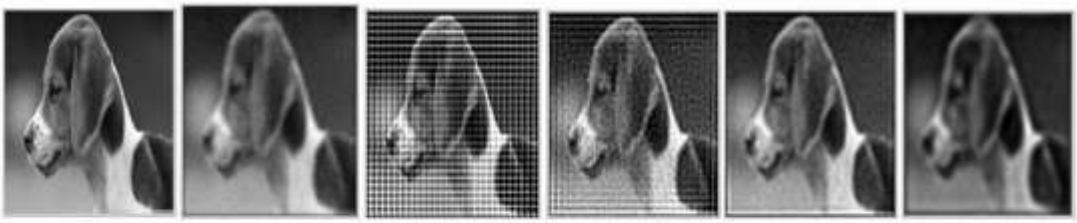

Figure1 Figure2 Figure3 Figure4 Figure5 Figure6

Figure 7 depicts the original image, whereas Figure 8 depicts a motion blurred and noisy version of it. When motion blur is present, the Wiener filter is used to recover the image shown in Figure 9. Figures 10 and 11 show the restored image using the CLS method, while Figure 12 shows the restored image using the modified LR method. Figures 11 and 12 also show the restored image using the LR method.

Figure 7 Figure 8 Figure 9 Figure 10 Figure 11 Figure 12

Table 1: PSNR Comparison in the presence of Gaussian Blur.

Filter Type	MSE	PSNR (dB)
Wiener Filter	1.0754e+004	17.9947
Constraint Least Square Filter	579.3914	47.2055
Lucy Richardson method	485.7005	48.9693
Modified Lucy Richardson method	421.8640	50.3784

Table 2: PSNR Comparison in the presence of Motion Blur.

Filter Type	MSE	PSNR (dB)
Wiener Filter	2.2033e+003	33.8482
Constraint Least Square Filter	1.1289e+003	40.5354
Lucy Richardson method	956.1066	42.1966
Modified Lucy Richardson method	882.0553	43.0027

In the presence of Gaussian blur& Motion blur, Table 1& Table 2 show the PSNR& MSE calculation between the non-degraded image and restored image using modified LR method, LR method, CLS method, and Wiener method in the presence of Gaussian blur& Motion blur.

5. Conclusion

The usual approach (wiener filter, regularized filter, Lucy- Richardson algorithm, and non-blind deconvolution) was utilized in this investigation. The optimal parameter for the wiener filter at noise variance (nv=103), the regularized filter at iteration (it=104), the Lucy- Richardson algorithm at iteration(it=1), and non-blind deconvolution at iteration(it=3) has been discovered. We concluded that Lucy-Richardson algorithm was superior to other approaches, and that our proposed methodology outperformed the original Lucy-Richardson algorithm, which had a better standard quality of SSIM.

Availability of data and material : Data can be provided based on the request

Competing interests : Not applicable

Funding : Not applicable

Authors' contributions : Two authors are involved in simulation of the datas and 2 authors are involved in manuscript writing.

Acknowledgements : Not applicable

REFERENCES

1. Gary J Sullivan, Jens-Rainer Ohm, Woo-Jin Han, ThomasWiegand, et al. Overview of the high efficiency video coding(hevc) standard. *IEEE Transactions on Circuits and Systemsfor Video Technology*, 22(12):1649–1668, 2012.

2. Kai Zeng, Tiesong Zhao, Abdul Rehman, and Zhou Wang.Characterizing perceptual artifacts in compressed videostreams. In *Human Vision and Electronic Imaging XIX*, volume9014, page 90140Q. International Society for Opticsand Photonics, 2014.

3. Guo Lu, Wanli Ouyang, Dong Xu, Xiaoyun Zhang, ZhiyongGao, and Ming-Ting Sun. Deep kalman filtering network forvideo compression artifact reduction. In *ECCV*, pages 568–584, 2018.

4. Ren Yang, Mai Xu, Tie Liu, Zulin Wang, and ZhenyuGuan. Enhancing quality for hevc compressed videos. *IEEETransactions on Circuits and Systems for Video Technology*,29(7):2039–2054, 2018.

5. Ren Yang, Mai Xu, Zulin Wang, and Tianyi Li. Multi-framequality enhancement for compressed video. In *CVPR*, pages6664–6673, 2018.
6. Chao Dong, Yubin Deng, Chen Change Loy, and XiaoouTang. Compression artifacts reduction by a deep convolutionalnetwork. In *ICCV*, pages 576–584, 2015.
7. Leonardo Galteri, Lorenzo Seidenari, Marco Bertini, and AlbertoDel Bimbo. Deep generative adversarial compressionartifact removal. In *ICCV*, pages 4826–4835, 2017.
8. Ying Tai, Jian Yang, Xiaoming Liu, and Chunyan Xu. Memnet:A persistent memory network for image restoration. In*CVPR*, pages 4539–4547, 2017.
9. Kai Zhang, WangmengZuo, Yunjin Chen, Deyu Meng, andLei Zhang. Beyond a gaussian denoiser: Residual learning ofdeepcnn for image denoising. *IEEE TIP*, 26(7):3142–3155,2017.
10. TianfanXue, Baian Chen, Jiajun Wu, Donglai Wei, andWilliam T Freeman. Video enhancement with task-orientedflow. *IJCV*, 127(8):1106–1125, 2019.
11. Shen, M.; Kuo, J. Review of Postprocessing Techniques for Compression Artifact Removal. J. Vis. Commun. Image Represent. **1998**, 9, 2–14.
12. Gonzalez, R.;Woods, R. Digital Image Processing; Pearson Education: London, UK, 2002.
13. List, P.; Joch, A.; Lainema, J.; Bjontegaard, G.; Karczewicz, M. Adaptive Deblocking Filter. IEEE Trans. Circuits Syst. Video Technol. **2003**, 13, 614–619.
14. Reeve, H.; Lim, J. Reduction of Blocking Effect in Image Coding. In Proceedings of the IEEE International Conference on Acoustics, Speech, and Signal Processing, Boston, MA, USA, 14–16 April 1983; pp. 1212–1215.
15. Liew, A.; Yan, H. Blocking Artifacts Suppression in Block-Coded Images Using Overcomplete Wavelet Representation. IEEE Trans. Circuits Syst. Video Technol. **2004**, 14, 450–461.
16. Foi, A.; Katkovnik, V.; Egiazarian, K. Pointwise Shape-Adaptive DCT for High-Quality Denoising and Deblocking of Grayscale and Coloe Images. IEEE Trans. Image Process. **2007**, 16, 1–17.
17. Chen, K.H.; Guo, J.I.; Wang, J.S.; Yeh, C.W.; Chen, J.W. An Energy-Aware IP Core Design for the Variable-Length DCT/IDCT Targeting at MPEG4 Shape-Adaptive Transforms. IEEE Trans. Circuits Syst. Video Technol. **2005**, 15, 704–715.
18. Lecun, Y.; Boser, B.; Denker, J.; Henderson, D.; Howard, R.; Hubbard, W.; Jackel, L. Backpropagation Applied to handwritten Zip code Recognition. Neural Comput. **1989**, 1, 541–551.
19. Hore, A.; Ziou, D. Image Quality Metrics: PSNR vs. SSIM. In Proceedings of the International Conference on Pattern Recognition, Istanbul, Turkey, 23–26 August 2010; pp. 2366–2369.
20. Silpa, K.; Mastani, A. New Approach of Estimation PSNR-B for De-blocked Images. arXiv**2013**, arXiv:1306.5293.
21. Yim, C.; Bovik, A. Quality Assessment of Deblocked Images. IEEE Trans. Image Process. **2011**, 20, 88–98.
22. Wang, Z.; Bovik, A.; Sheikh, H.; Simoncelli, E. Image Quality Assessment: From Error Visibility to Structural Similarity. IEEE Trans. Image Process. **2004**, 13, 600–612.
23. H. Chang, M.K. Ng, T. Zeng, Reducing artifacts in JPEG decompression via a learned dictionary. IEEE Trans. Signal Process. 62(3), 718–728 (2014)
24. R. Rothe, R. Timofte, L. Van, in IEEE International Conference on Image Processing. Efficient regression priors for reducing image compression artifacts (IEEE International Conference on Image Processing, 2015), pp. 769-777
25. A. Foi, V. Katkovnik, K. Egiazarian, Pointwise shape-adaptive DCT for highquality denoising

and deblocking of grayscale and color images. IEEE Trans. Image Process. 16(5), 1395 (2007)
26. M.T. Wu, Wavelet transform based on Meyer algorithm for image edge and blocking artifact reduction. Inf. Sci. 474, 125–135 (2019)

27. C. Dong, Y. Deng, C.L. Chen, et al., in IEEE International Conference on Computer Vision. Compression artifacts reduction by a deep convolutional network (IEEE International Conference on Computer Vision, 2016), pp. 576–584
28. Z. Wang, L. Ding, S. Chang, et al., in IEEE Conference on Computer Vision & Pattern Recognition. D3: Deep dual-domain based fast restoration of JPEGcompressed images (2016)
29. X. Wang, P. Zhang, Y. Zhang, et al., Deep Intensity Guidance Based Compression Artifacts Reduction for Depth Map. J. Vis. Commun. Image Represent. 57, 234-242 (2018)
30. Ledig C, Wang Z, Shi W, et al. Photo-Realistic Single Image Super-Resolution Using a Generative Adversarial Network 2016 arXiv.org.
31. A. Radford, L. Metz, S. Chintala, Unsupervised representation learning with deep convolutional generative adversarial networks. Comput. Sci. (2015) https://arxiv.org/pdf/1511.06434.pdf
32. P. Isola, J. Zhu, T. Zhou, A.A. Efros, Image-to-image translation with conditional adversarial networks, 2017 (IEEE Conference on Computer Vision and Pattern Recognition (CVPR), Honolulu, 2017), pp. 5967–5976
33. I.J. Goodfellow, J. Pouget-Abadie, M. Mirza, et al., Generative adversarial networks. Adv. Neural Inf. Proces. Syst. 3, 2672–2680 (2014)
34. M. Bertero and P. Boccacci, “A simple method for the reduction of boundary effects in the Richardson-Lucy approach to image deconvolution,”Astronomy and Astrophysics,Vol. 437,pp. 369-374, July 2005.
35. Wei-Gang Chen and Runyi Yu et al., Neural Network-Based VideoCompression Artifact ReductionUsing Temporal Correlation andSparsity Prior Predictions, Aug (2020)
36. K.G. Revathi, D. Poornima And BelsamJeba Ananth, A Novel Video Compression Then Restoration Artifact Reduction Method Based on Optical Flow Consistency to Improve the Quality Of The Video (2020)

*e*ISSN1303-5150